POLISH MARITIME RESEARCH 1 (97) 2018 Vol. 25; pp. 24-32
10.2478/pomr-2018-0004

APPLICATION OF VORTEX FLOW MODEL IN PROPELLER-STATOR SYSTEM DESIGN AND ANALYSIS

Przemysław Król
Ship Design and Research Centre, Gdańsk, Poland
Gdańsk University of Technology, Poland
Tomasz Bugalski
Ship Design and Research Centre, Gdańsk, Poland

ABSTRACT

The paper covers basics of the vortex model used for propeller-stator systems. The outline of the design algorithm is given and the results of its application are shown. The designed propeller-stator system was the subject of model tests run at the CTO model basin and cavitation tunnel. Stator's influence on the delivered power required by the propeller and its revolution rate has been examined by conducting self-propulsion tests with and without stator. The tests performed in the cavitation tunnel revealed only weak tip vortex cavitation on the propeller. No cavitation was observed on the stator at the design point. A wide range of the performed tests allowed the authors to identify details of the developed theory which will require further improvement.

Keywords: Propeller, Wake improving device, Upstream stator, Cavitation,V ortex lattice method

FLUID MOTION MODEL

The equations describing the motion of real fluid are almost impossible to solve – integrating them analytically is possible only for some simplified cases. Due to this, the ideal (incompressible, inviscid) fluid model is still in wide use. Within this model, the mass conservation equation is:

$$div\ \vec{U} = 0 \tag{1}$$

and the momentum conservation equation (Euler equation) is:

$$\frac{D\vec{U}}{Dt} = \vec{F} - grad\ p \tag{2}$$

Although significantly simplified, these equations are still hardly solvable. However, it is possible to introduce a scalar function of velocity potential:

$$grad\ \varphi = \vec{U} \tag{3}$$

Applying this potential definition to the mass conservation equation leads to the Laplace equation:

$$div\ \vec{U} \equiv \Delta\varphi = 0 \tag{4}$$

The above equation is linear, which means that the superposition of its individual solutions is still the equation's solution. A special class of individual, elementary solutions of the Laplace equation is known as hydrodynamic singularities.

Each type of hydrodynamic singularities induces a specific velocity field in the surrounding area. In general case, it may be expressed as:

$$\vec{U}_{ind}(\vec{r}) = A(\vec{r})\vec{e}(\vec{r}) \tag{5}$$

where A is the scalar value depending on the type of singularity, its strength, and the distance to the calculation point. The unit vector $\boldsymbol{e}$ is dependent only on the type of singularity and its position with respect to the calculation point.

The use of hydrodynamic singularities is a convenient concept for solving flow problems with discrete panel approach. The surface of the body immersed in the flow is divided into small pieces, and at each of them the kinematic boundary condition for ideal fluid motion is demanded:

$$\vec{U}_{total}(\vec{r}) \bullet \vec{n}(\vec{r}) = 0 \tag{6}$$

Singularities of known type are distributed over the reference surface (which does not necessarily have to coincide with the surface of the body immersed in the flow). It is important to have a number of unknowns describing the singularity strength distribution, and the same number of panel control points at which the boundary condition is enforced. It allows to construct the system of linear equations and exactly determine the strengths of individual singularities.

It is noteworthy that the hydrodynamic singularities compose the solution for ideal fluid motion and, consequently, no viscous effects are taken into account. In most applications, viscous drag is calculated based on simplified formulas or the boundary layer analysis. Separation phenomena are omitted, or just signalized. Especially the latter may lead to unrealistic results, such as the well-known d'Alembert paradox.

Despite these limitations, the singularity method is quite useful – especially for slender bodies, such as hydrofoils for instance, where separation phenomena are in most cases of minor importance.

DESIGN VORTEX MODEL

ALGORITHM OUTLINE

The design algorithm is arranged as chain of subsequent logical steps. The starting point is the assumption on stator blade circulation distribution. It allows to determine the stator induced velocity field in propeller plane and the stator drag force, which are basic input data for further steps.

For the assumed stator circulation distribution, an optimum propeller is designed. Its initial design is prepared using the lifting line algorithm. Its only purpose is to evaluate the system efficiency that is expected to be achieved in the prescribed conditions. If it is satisfactory, the propeller design algorithm proceeds to a more detailed phase.

Once the propeller geometry is designed, it is possible to analyse it using the lifting surface model. One of its outputs is the propeller induced velocity field in stator plane. It serves as the input for subsequent stator design.

The block diagram presents the outline of the algorithm adopted for propeller–stator system design:

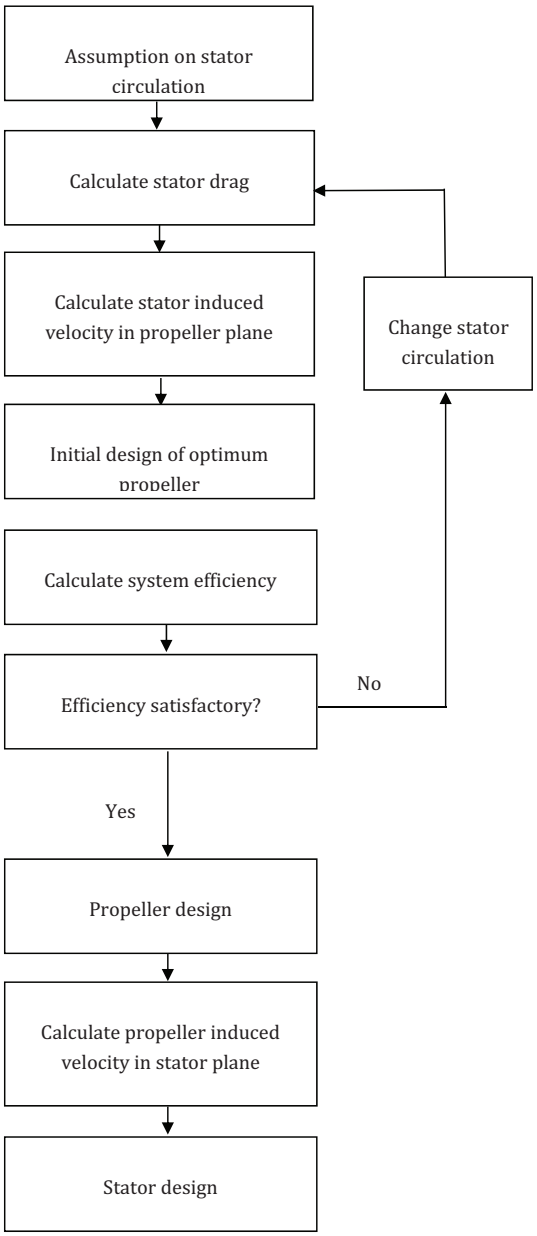

Fig. 1. *Block diagram of the design algorithm*

A detailed description of each step of the outlined algorithm is given further in the paper.

CIRCULATION DISTRIBUTION

Despite the fact that flow phenomena existing around the propeller-stator system are very complex, simple singularity models can still be successfully used [1]. From a wide family of singularity models, two were adopted in this work, which were: the lifting line model for the design task, and the lifting surface for the analysis task. In this section the former model is described.

The singularity model used for the design task is very simple. It replaces propeller and stator blades with lifting lines of variable radial circulation distribution. As it is the

initial theory, some additional simplifications have been introduced. First of all, the stator is assumed to be lightly loaded. Consequently, the deformation of its vortex wake is neglected and the wake is assumed to follow the external velocity field. This assumption turned out to be acceptable for low and moderate values of total bound circulations over the stator blade.

The circulation distribution along stator blades is a priori assumed to have an elliptical shape. This decision is based on the well-known conclusion from the Prandtl lifting line theory on the induced drag minimum for elliptical distribution of bound circulation.

The propeller itself is assumed to be moderately loaded, and the propeller induced velocities are taken into account while calculating the pitch of the propeller vortex wake. It is assumed to form a true helical surface, whose shape is determined upon the total velocity field, taking into account the external wakefield, and stator and propeller induced velocities. However, the propeller blades are replaced with lifting lines of radially variable bound circulation distribution. A general view of the actual vortex model is given in Fig. 2.

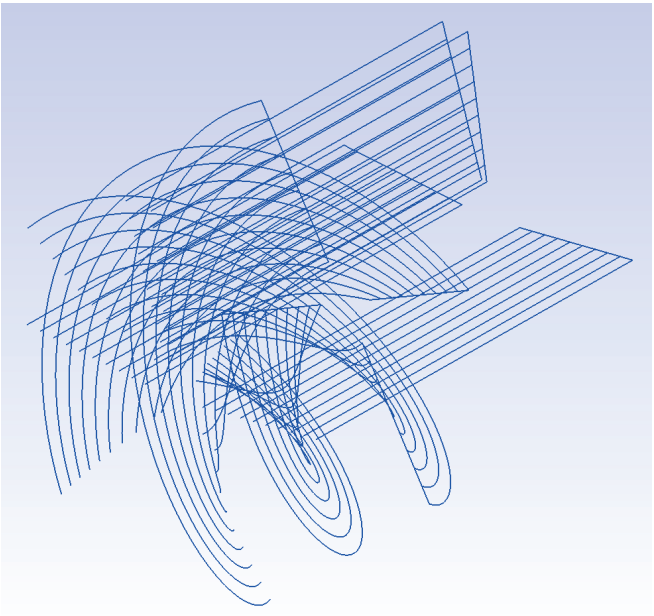

Fig. 2. Propeller and stator lifting line representation

The circulation distribution along the propeller blade does not follow any additional assumption – it is determined as in the classical lifting line algorithm for propeller design making use of Goldstein factors.

Since the deformations of the stator and propeller vortex wakes are neglected, there is no need for an iterative process of stator-propeller coupling. It must be underlined, however, that this assumption is rather crude and may lead to significant discrepancies between theoretical and experimental results - especially for higher propeller/stator loads.

STATOR INDUCED VELOCITIES

The very first step of the design task is to determine the velocity field induced by the stator in the propeller plane. As mentioned before, it is assumed that the bound circulation distribution over stator blades is elliptical. The free stator vortices are assumed to form flat surfaces, parallel to the external flow vector. Upon this assumption it is easy to determine the stator induced velocity field wherever around it. However, it is possible to make further simplification of calculations, as the mean velocities at each radius are the same for one lifting line with maximum bound circulation Γ and for the set of N lifting lines of the accumulated maximum bound circulation equal to Γ. This is true as long as all these lifting lines have the same shape of bound circulation distribution and the same blade length.

It is convenient to express stator induced velocities as coefficients:

$$c = u \cdot \frac{L}{\Gamma_{MAX}} \tag{7}$$

where u is the induced velocity, L is the length of the stator blade and Γ_{MAX} is the maximum value of bound circulation over the lifting line. When using the single lifting line approach, it shall be set equal to the accumulated value of maximum bound circulations values of all stator blades.

At the stage of propeller stator system design, the most important value to be known is the mean value of stator induced tangential velocity at each propeller radius. The induced velocities are in general complex functions of circulation distribution shape and position with respect to the lifting line. In the case of mean tangential components, they turned out to be very insensitive to the axial distance between propeller and stator planes; for a distance larger than 3L their changes are negligible. For further calculations, the values of c coefficients determined for the relative distance of 0.5L were used.

Since the viscous effects are neglected, the mean value of axial induced velocity is equal to zero for each radius. Due to the presence of the viscous wake behind a body in the real fluid, it shall have a small negative value. However, there is no simple and reliable method to determine it and that is why this effect has been neglected.

Within the flat wake assumption, the values of c coefficients are independent on Γ_{MAX} and once determined they can be used for seeking for the optimum value of stator bound vorticity. From the propeller point of view, the best approach is to apply as high stator circulation as possible. However, the stator itself generates a hydrodynamic drag. Its value is judged based on the simplified formula:

$$D = 1.5 \frac{L^2}{\frac{\pi\rho}{2} V^2 L^2} \tag{8}$$

where L is the lifting force determined using the lifting line model for stator blades, and V is the ship's advance speed. This formula is based on the induced drag experienced by a finite span hydrofoil with elliptical loading distribution operating in the ideal fluid.

After prescribing the arbitrarily chosen value of Γ_{MAX} for the whole stator, the initial propeller design is made. If the system efficiency, defined as:

$$\eta = \frac{(T_{PROP} - D_{STATOR})V}{2\pi nQ} \tag{9}$$

is satisfactory, then the stator circulation value is accepted as the design parameter.

PROPELLER DESIGN

The propeller design makes use of the very classic lifting line algorithm, supplemented with lifting surface correction factors [2]. The only difference, compared to conventional applications, is taking into account stator induced mean tangential velocities when calculating advance angles and coefficients.

At this stage, the propeller induced axial velocities in stator plane are calculated with the lifting surface software. Stator's presence is taken into account by applying stator induced tangential velocities in propeller plane. The propeller induced velocities are later used at the stator design stage.

STATOR DESIGN

The stator geometry was designed making use of an algorithm very similar to the classical propeller lifting line method [2]. Slight changes were necessary with respect to the local inflow angle definition, as the stator is not rotating.

The stator design starts with determining the value:

$$C_L b = 2\frac{\Gamma}{V_W} \tag{10}$$

where C_L is the lift force coefficient, b is the blade width, Γ is the local bound circulation, and V_W is the local total velocity:

$$V_W = \sqrt{V_A^2 + V_T^2} \tag{11}$$

where V_T and V_A are the total tangential and axial velocities, respectively. They can be written as:

$$V_W = \sqrt{\left(V(1-w) + u_{A,PS} + u_{A,SS}\right)^2 + u_{T,SS}^2} \tag{12}$$

where V is the ship's advance speed, w is the wake fraction at the considered position, $u_{A,PS}$ is the axial velocity induced by the propeller in stator plane, and $u_{A,SS}$ and $u_{T,SS}$ are, respectively, the axial and tangential velocity induced by the stator in its plane.

The stator induced velocities for formula (12) are determined with the discrete lifting line method, while the propeller induced axial velocity is determined with the discrete lifting surface analysis software, as mentioned before.

As the propeller rotates with respect to the stator, its induced velocity is taken as mean value at considered radius. However, the wake fraction w and the stator induced velocities $u_{A,PS}$ and $u_{T,SS}$ are functions of two coordinates: angle (defining the stator blade angular position with respect to the propeller shaft axis), and radius (being the stator blade radius).

Subsequently, the local cavitation number is calculated:

$$\sigma = \frac{p_A - p_v + \rho(h - l_z)g}{\frac{1}{2}\rho V_W} \tag{13}$$

The local blade thickness is initially assumed to be equal to:

$$t = 0.02L \tag{14}$$

To determine the blade width-to-thickness ratio, cavitation diagrams are used. This allows us to determine the blade width b as:

$$b = t\left(\frac{b}{t}\right) \tag{15}$$

and to calculate directly the local lift force coefficient. The ideal attack angle is determined as:

$$\alpha_0 = 0.0245 C_L \tag{16}$$

Now, the local inclination angle of stator blade is given as:

$$\varphi = \arctan\left(\frac{V_T}{V_A}\right) + \alpha_0 \tag{17}$$

and the local camber value is:

$$f = 0.0679 f \cdot C_L \tag{18}$$

After determining the stator geometry, the stator drag is estimated from the formulas:

$$C_D = 0.008 + 1.7\alpha_0^2 \tag{19}$$

$$\frac{dD}{dl} = \frac{1}{2}\rho V_W^2 b \qquad (20)$$

where C_D is the local drag force coefficient and dD/dl is the drag force derivative along stator blade span. The overall stator drag is the sum of particular blade drag forces, obtained by integrating dD/dl over the span.

The abovementioned method for drag force determination is also applied to the propeller.

VORTEX MODEL ANALYSIS

The separate vortex model software was applied for the analysis task, upon the classical vortex lattice approach [2], [3], [4]. The first of them is used for analysing the propeller alone. It is meant for determining propeller open water loading characteristics. In this software, the propeller vortex wake is allowed to deform under its own induced velocities by convective manner. The propeller hub is also included, which allows the user to achieve reasonable results for high values of advance coefficient. The external wake field may be taken into account.

Sample results of propeller calculations with this software are given in Table 1:

Tab. 1. Representative results of lifting surface calculations

J	KT_{emp}	KT_{cal}	$10KQ_{emp}$	$10KQ_{cal}$	η_{emp}	η_{cal}
0.500	0.285	0.283	0.477	0.464	0.489	0.485
0.700	0.200	0.213	0.360	0.361	0.632	0.657
0.833	0.146	0.160	0.280	0.283	0.692	0.751
0.900	0.120	0.131	0.239	0.240	0.725	0.783
1.100	0.034	0.034	0.106	0.097	0.575	0.614

These results were obtained for a three-bladed symmetrical outline propeller [5]. The here presented lifting surface results are also representative for other propellers. However, better agreement for higher loads than for the design point is rather specific for this particular propeller. The overestimated efficiency values are likely to result from the underestimated value of viscous drag in the considered case.

This vortex lattice approach was considered capable of giving acceptable accuracy to be used for analysing propeller-stator systems. It is used for determining hydrodynamic characteristics of the propeller and the propeller induced velocity field.

Another piece of software was developed as the modification of the previous one. Initially, the vortex wakes were fixed to have certain rigid shape and no iterative relaxation was used. Some attempts were made to allow only the propeller vortex wake to deform, with the stator vortex fixed as flat surface. However, such a half-deformative approach turned out to lead to highly overestimated values of generated thrust force, so it was given up.

The first step of the VLM analysis comprises determining the stator blade circulation distribution. It is done based only on the external velocity field, while neglecting the presence of the propeller. Once the stator circulation distribution is known, the mean value of the velocity vector (given in the cylindrical coordinate system) is calculated in the propeller plane for each radius (assuming that axial variation of stator induced velocities over propeller axial length is negligible). With this velocity field known, the propeller circulation distribution is determined and then the stator circulation distribution with propeller induced velocities is taken into account. This propeller-stator circulation coupling is an iterative process, but it converges very quickly – in 2–3 iterations.

4 APPLICATION

The ship Nawigator XXI was used as the test case for the above described algorithm. However, the newly designed system was not applied in full scale. The original propeller, which was the four-bladed CP469, served as the stock propeller during self-propulsion tests. Then, a decision was made that a new propeller expected to cooperate with the upstream stator shall be a five-bladed one. The input parameters for the design task were as following:

- design speed: V = 12.9 knots;
- propeller shaft rotation n = 257.9 rpm;
- required thrust T = 124kN ;
- propeller diameter D = 2260mm;
- stator blade length L=1130mm;
- number of propeller blades Z = 5;
- number of stator blades N=4;
- propeller shaft immersion h = 3500mm;
- average wake fraction coefficient w = 0.362;

Fig. 3. and Fig. 4 show 3D models of the designed propeller CP745 and stator ST001, respectively.

Main particulars of the propeller are:

- expanded area ratio EAR = 0.7592;
- mean pitch ratio P/D = 0.7500;
- skew angle SKA = 15.85deg.

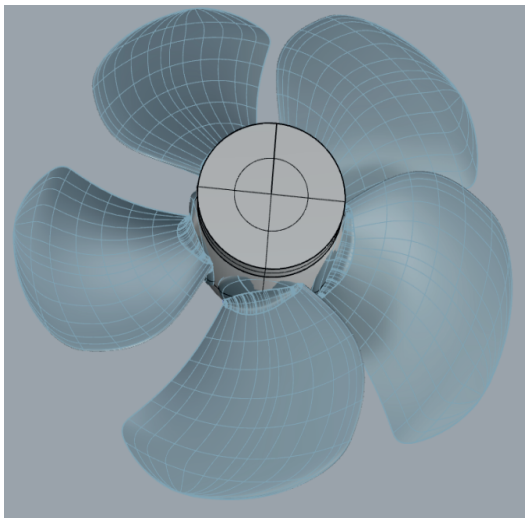

Fig. 3. Designed controllable pitch propeller CP745

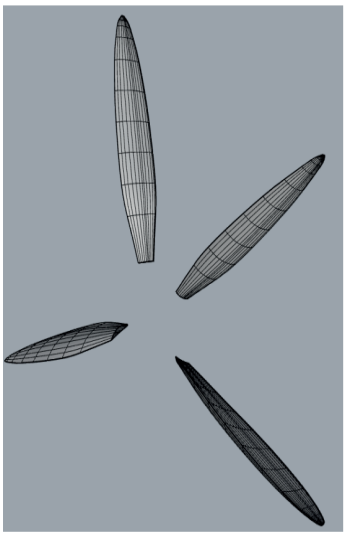

Fig. 4. Designed stator ST001

The presented propulsion system was manufactured in model scale and tested. The tests were performed for two arrangements - with and without stator:

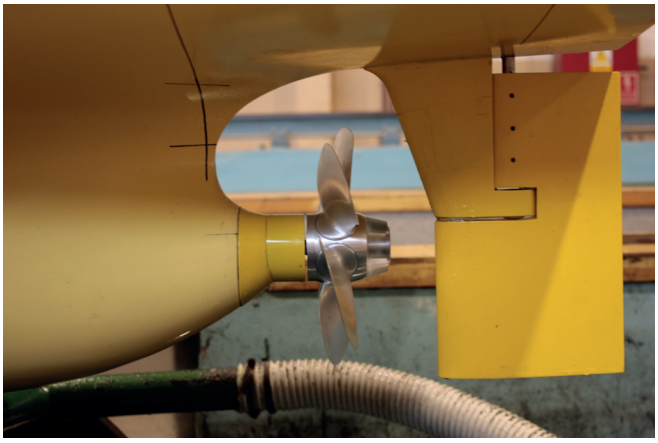

Fig. 5. Self-propulsion test arrangement without pre-swirl stator

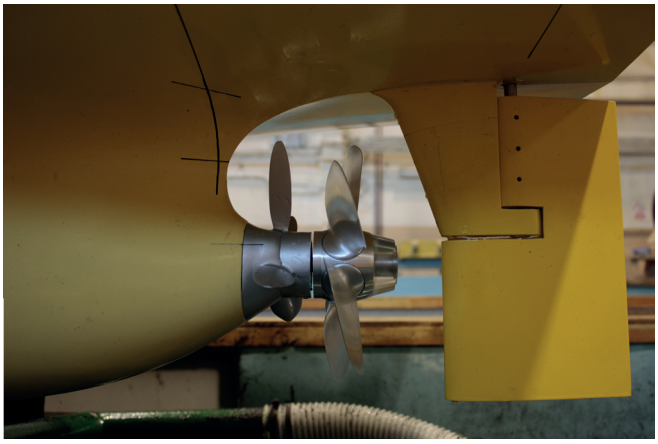

Fig. 6. Self-propulsion test arrangement with pre-swirl stator

All models used in the tests were manufactured in the Ship Hydromechanics Division of CTO S.A. The aft bulb of the hull model was cut off and replaced with exchangeable ending. The latter was manufactured in two versions: one reproducing the original aft bulb geometry and the other – with stator blades mounted.

WAKEFIELD MEASUREMENT

The wakefield was measured behind the hull model without and with stator, Fig. 7 and Fig. 8, respectively.

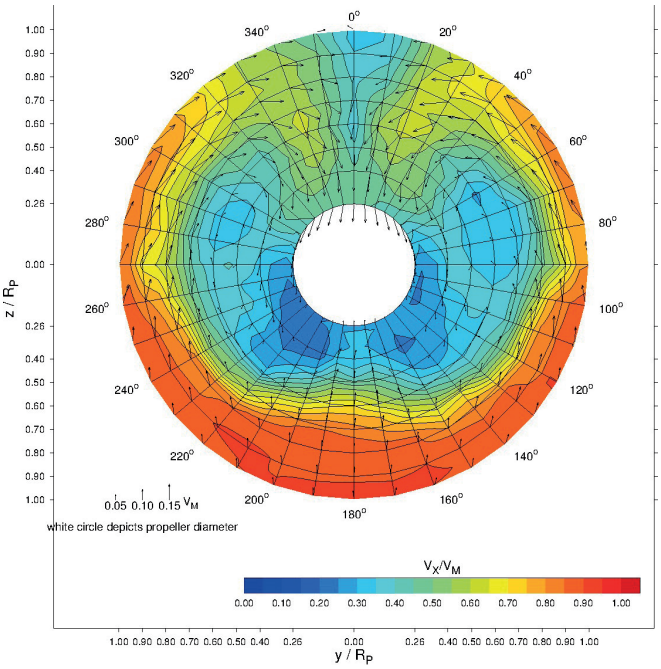

Fig. 7. Non-uniform velocity field behind hull model without stator

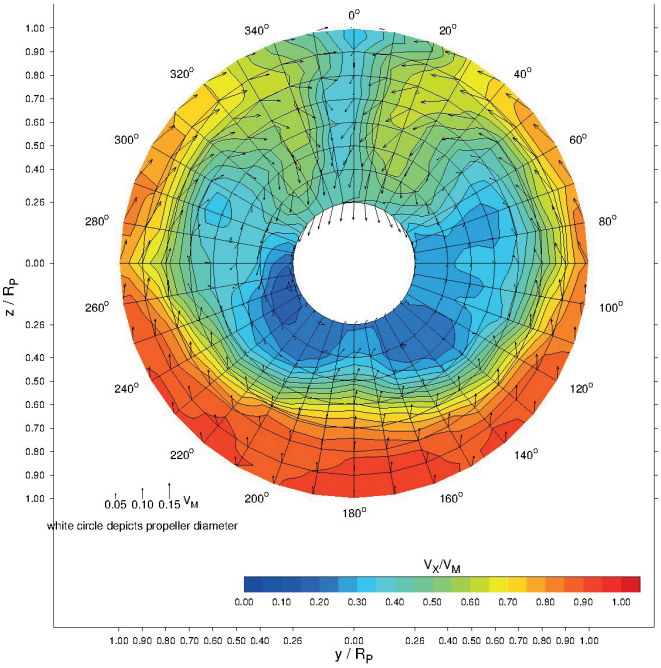

Fig. 8. Non-uniform velocity field behind hull model with stator

The differential wakefield is shown in Fig. 9. It presents the difference between velocity fields measured behind the hull with and without stator.

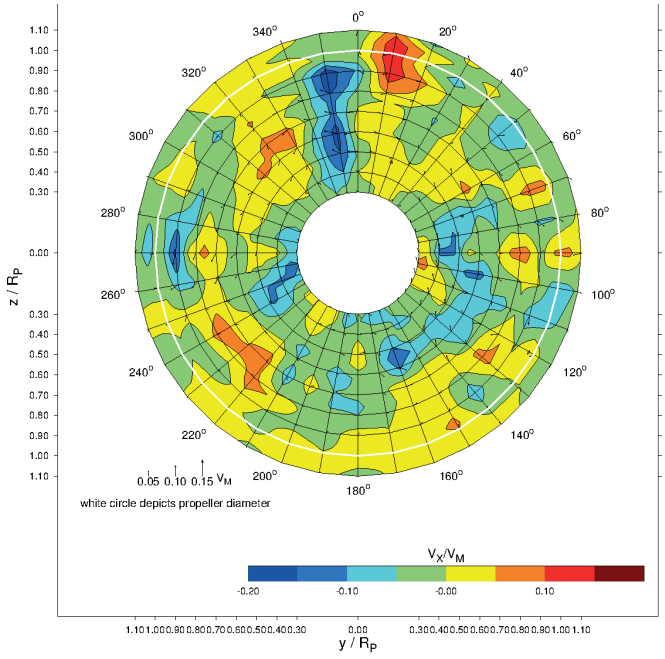

Fig. 9. Differential wakefield

The mean value of the differential wakefield is zero (within the measuring tolerance). It confirms the conclusion from the lifting line model that the stator, in general, does not influence the average axial velocity in the propeller disc.

However, there is no clear tendency in local axial velocity contribution with respect to particular stator blades (angular positions: 60, 120, 260 and 350 degrees). We believe that it results from the fact that the stator was designed to cooperate with the propeller. The inflow angles on the stand-alone stator are substantially different, and so is the stator's circulation distribution. This conclusion is not contradictory to the statement on average axial velocity, as it is independent of the lifting line load distribution.

The differential tangential component of the wakefield is given in Fig. 10.:

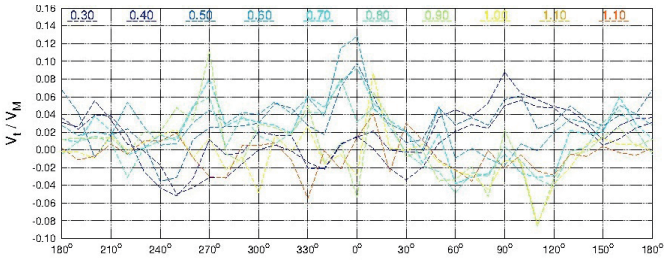

Fig. 10. Differential wakefield tangential component

It can be clearly seen that for most part of the measuring area, there is notable positive contribution from the stator to the tangential velocity component. However, since the stator load without the cooperating propeller is much lower than the design one, the tangential induced velocities are also small. Nevertheless, the effect is as desired, and the stator introduces a non-zero tangential velocity component.

SELF-PROPULSION TEST

The self-propulsion test was performed in two configurations: with and without stator. The test results for these two configurations are compared in Table 2.

Tab. 2. Stator influence on propulsion prediction

V[kn]	PD_o [kW]	$n_{w/o}$ [rpm]	PD_w [kW]	n_w [rpm]
9.00	225	173.4	218	169.6
10.00	334	196.6	322	192.6
11.00	504	224.6	475	218.3
12.00	716	251.5	680	245.1
13.00	1123	289.3	1077	282.9

It can be clearly seen that the stator's presence significantly affected the propulsion system characteristics. The stator's presence allowed to reduce both the required power delivered to the propeller, and the revolution rate. This brings not only economical gains, thanks to the reduction in fuel consumption, but also decreases the risk of cavitation.

CAVITATION TEST

The designed system also underwent the cavitation test. The input parameters for this test were: KT=0.253 and σ=2.622. The nominal wakefield in propeller plane was reproduced with the use of a dummy model equipped with appropriate wire mesh.

The nominal wakefield applied for the cavitation test was that measured behind the hull without stator. As the stator was present in the testing arrangement, it was pointless to reproduce the wakefield measured behind the hull with the stator mounted. Fig. 11 compares the nominal wakefields measured in the towing tank and in the cavitation tunnel. The thick blue line refers to the towing tank wakefield, and the thin purple line refers to the cavitation tunnel.

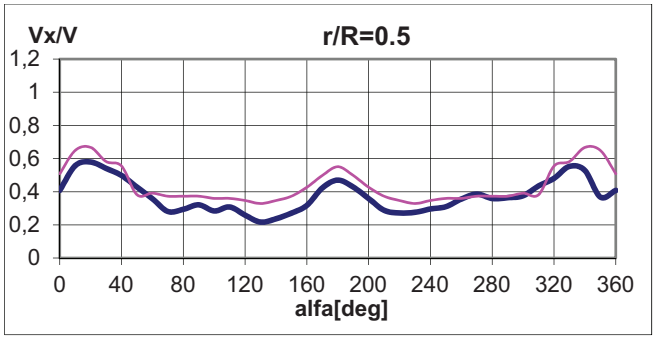

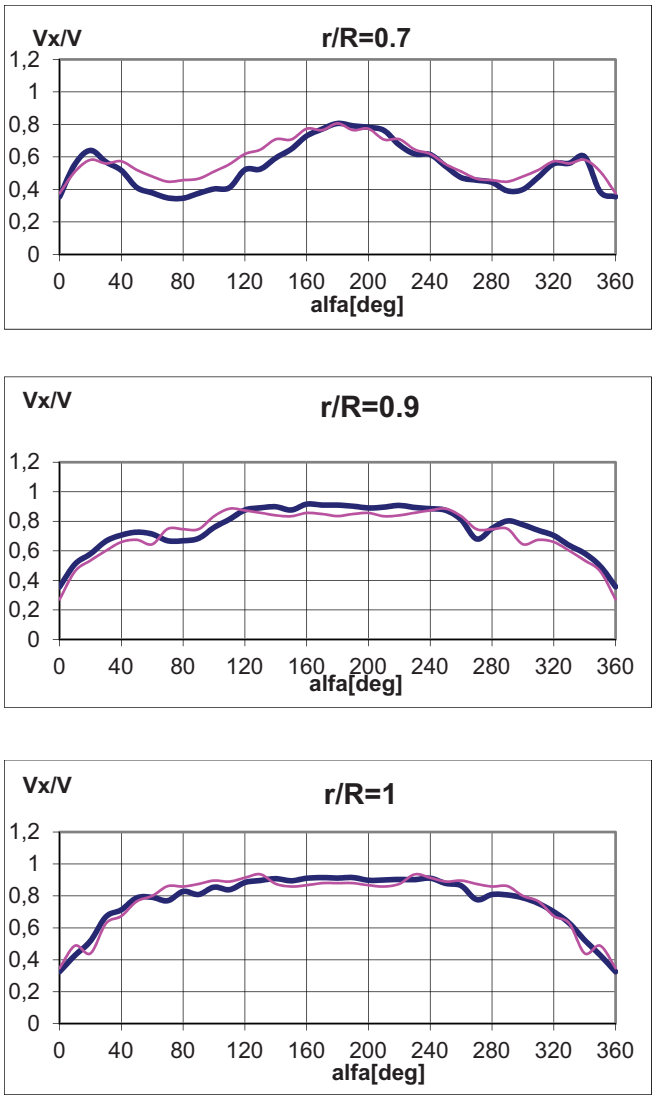

Fig. 11. Wakefield axial component

Cavitation observation revealed a weak, but stable cavitating tip vortex.

The presence of the tip vortex on the propeller is likely to result from an error made within the assumed designed condition saying that the stator blade should have the same length as the propeller radius. This error leads to the intersection of the stator tip vortex with the propeller tip, which may provoke increased cavitation in this region.

No cavitation was observed on the stator blades. An attempt to determine stator's cavitation limits failed, as the wire mesh applied for modelling the wakefield started to cavitate long before any form of cavitation became visible on the stator.

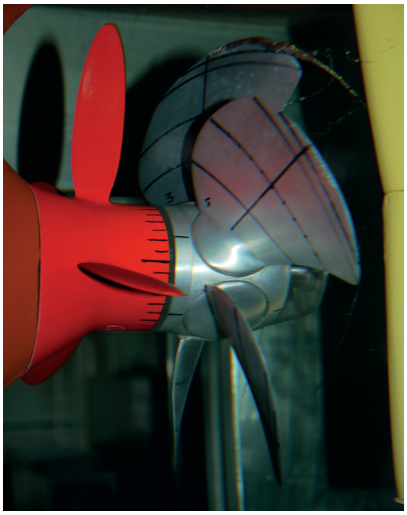

Fig. 12. Cavitation observation

TIP VORTICES

Additional cavitation test was performed to visualize propeller tip vortices. The rotational speed of the propeller was fixed and the advance speed of water in the cavitation tunnel was decreased to increase propeller load. The pressure in the test section was kept at such a level as to obtain stable cavitating tip vortices.

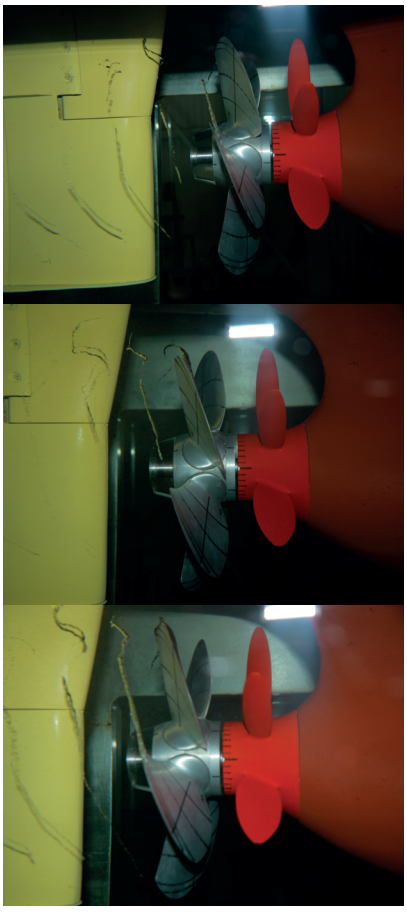

Fig. 13. Tip vortices for KT (from up to down): 0.191; 0.211; 0.243.

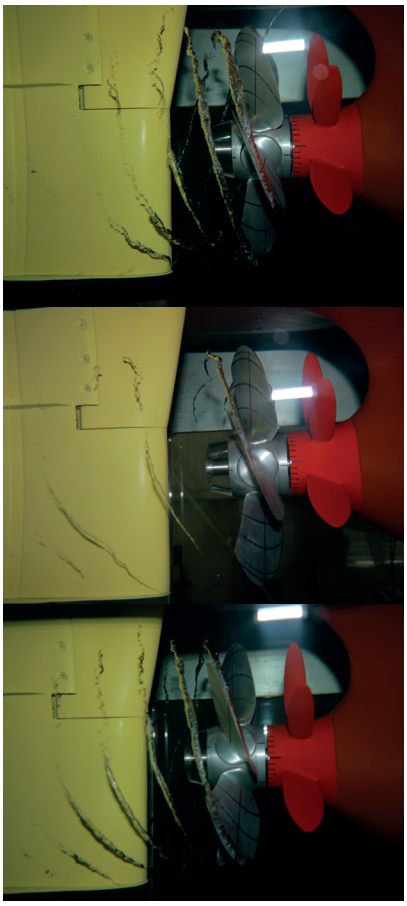

Fig. 14. Tip vortices for KT (from up to down): 0.243; 0.296; 0.361

This test was performed to collect the reference material for further validation of vortex wake relaxation procedures in the VLM-base propeller analysis software.

CONCLUSIONS AND FURTHER WORK

The actual vortex model is very robust. However, due to the applied simplifications it does not give very accurate results. The main reason for this was identified as neglecting the free vortex wake deformation. This effect is to be included in future development of the theory. Moreover, it is planned to replace the simple lifting line algorithm used for determining the pitch and camber of both propeller and stator with the lifting surface model. The presented method can be applied in designing propeller stator systems. However, the designed systems should be carefully tested in model scale, especially in cases of high propeller-stator loads, when the behaviour of vortex systems may significantly differ from that within the adopted model.

ACKNOWLEDGEMENT

Materials and concepts presented in this paper were elaborated within the INRETRO project realized as the European ERA-NET venture within the MARTEC II framework. The financial support by the national funding associations is gratefully acknowledged.

BIBLIOGRAPHY

1. Kerwin, J., Coney, W., Hsin, C.: *Hydrodynamic Aspects of Propeller/Stator Design*, The Society of Naval Architects and Marine Engineers, 1988.
2. Greeley, D., Kerwin, J.: *Numerical Methods for Propeller Design and Analysis in Steady Flow*, Transactions of Society of Naval Architects & Marine Engineers, 1982.
3. [3] Jarzyna, H., Koronowicz, T., Szantyr, J.: *Design of Marine Propellers - Selected Problems*, Wrocław: Ossolineum, 1996.
4. [4] Bugalski, T., Szantyr, J.: *Numerical Analysis of the Unsteady Propeller Performance in the Ship Wake Modified by Different Wake Improvement Devices*, Polish Maritime Research, 2014.
5. [5] Koyama, K.: *Comparative calculations of propellers by surface panel method - workshop organized by 20th ITTC Propulsor Committee*, Papers of Ship Research Institute, 1993.

CONTACT WITH THE AUTHORS

Przemysław Król
e-mail: przemyslaw.krol@cto.gda.pl
Ship Design and Research Centre
Szczecinska 65, 80-392 Gdańsk
Poland
Faculty of Mechanical Engenieering
Gdansk University of Technology
Narutowicza 11/12, 80-233 Gdańsk
Poland

Tomasz Bugalski
e-mail: tomasz.bugalski@cto.gda.pl
Ship Design and Research Centre
Szczecinska 65, 80-392 Gdańsk
Poland